Virchows Arch (2001) 438:280–288
DOI 10.1007/s004280000353

ORIGINAL ARTICLE

Y. Sadahira · K. Akisada · T. Sugihara · S. Hata
K. Uehira · N. Muraki · T. Manabe

Comparative ultrastructural study of cytotoxic granules in nasal natural killer cell lymphoma, intestinal T-cell lymphoma, and anaplastic large cell lymphoma

Received: 17 August 2000 / Accepted: 3 October 2000 / Published online: 8 December 2000
© Springer-Verlag 2000

Abstract Comparative immunohistochemical and ultrastructural studies were performed on five nasal natural killer (NK) cell lymphoma cases, two intestinal T-cell lymphoma cases, and eight anaplastic large cell lymphoma (ALCL) cases to clarify morphological differences in cytotoxic granules among these cytotoxic lymphomas. Nasal NK-cell lymphomas and intestinal T-cell lymphomas had fine azurophilic granules and displayed dot-like immunostaining of granzyme B- and T-cell intracellular antigen 1 (TIA-1), predominantly in the central area of the cytoplasm. Ultrastructurally, these NK-cell lymphomas and intestinal T-cell lymphomas had two types of cytotoxic granules, type-I granules (dense core granules) and type-II granules (multivesicular bodies), which have been demonstrated in normal large granular lymphocytes in peripheral blood. However, ALCLs did not have azurophilic granules, and only type-II cytotoxic granules were found ultrastructurally, even though they showed similar dot-like immunostained patterns of granzyme B and TIA-1, as seen in NK-cell lymphomas and intestinal T-cell lymphomas. Immunoelectron microscopy revealed that TIA-1 was primarily located at the periphery of the cytoplasmic granules in the NK-cell lymphoma and ALCL cases. These findings suggest that malignant lymphomas with a cytotoxic phenotype can be divided into two types, (azurophilic granule)$^+$, (type-I granule)$^+$, (type-II granule)$^+$ lymphomas and (azurophilic granule)$^-$, (type-I granule)$^-$, (type-II granule)$^+$ lymphomas.

Keywords Cytotoxic granules · NK-cell lymphoma · Ultrastructure

Y. Sadahira (✉) · S. Hata · N. Muraki · T. Manabe
Department of Pathology, Kawasaki Medical School,
577 Matsushima, Kurashiki 701–0192, Japan
e-mail: sadapath@med.kawasaki-m.ac.jp
Tel.: +81-86-4621111, Fax: +81-86-4621199

K. Akisada
Department of Otorhinolaryngology, Kawasaki Medical School,
Kurashiki, Japan

T. Sugihara
Division of Hematology, Department of Medicine,
Kawasaki Medical School, Kurashiki, Japan

K. Uehira
Electron Microscopic Center, Kawasaki Medical School,
Kurashiki, Japan

Introduction

Cytotoxic lymphocytes comprised of a heterogeneous population, including natural killer (NK) cells and cytotoxic T lymphocytes, contain cytotoxic molecules, such as perforin, granzyme B, and T-cell intracellular antigen 1 (TIA-1; GMP-17) [1, 2, 8, 17, 29, 34]. These molecules have been implicated in cytolytic processes leading to apoptosis of target cells by being released from cytotoxic granules that display two morphologically distinct types. Type-I granule (dense core granule) is comprised of electron dense core domain of homogeneous appearance, surrounded by a thin cortex of vesicles or lamellae, and type-II granule (multivesicular body) is comprised of a multivesicular domain, which contains multiple small vesicles [5, 16, 28]. The classification into types reflects the relative proportion of these two domains in each granule. Immunoelectron microscopy has revealed that perforin and granzyme B are located in the dense core domains and multiple vesicles [16, 29] and TIA-1 is predominantly located in the membrane part of both types of granules [1, 2].

Malignant lymphomas that express cytotoxic molecules have recently been recognized using immunohistochemical methods. These include heterogeneous clinicopathologic entities, for example, NK-cell lymphoma [4, 10, 13], intestinal T-cell lymphoma [7, 9], γδ T-cell lymphoma [31], and anaplastic large cell lymphoma (ALCL) with or without anaplastic lymphoma kinase (ALK) expression [12, 14, 27]. Nasal NK-cell lymphomas are characterized by proliferation of atypical cells with cytoplasmic azurophilic granules and immunopositivity for CD2 and CD56 [20]. Intestinal T-cell lymphomas are phenotypically distinct and are thought to be derived

from intraepithelial T lymphocytes that display cytotoxic functions [6, 7]. Importantly, these lymphomas often show aggressive clinical behavior [24]. The cellular origin of ALCLs remains unknown, but these lymphomas may originate from $CD4^+$ or $CD8^+$ cytotoxic T cells, because they often express these T-cell markers and cytotoxic molecules [15, 23]. In particular, ALK-positive ALCLs more often express cytotoxic molecules than ALK-negative ALCLs, whereas the former usually follows an indolent clinical course [12, 14, 27].

Although the cytotoxic granules have been ultrastructurally demonstrated in each reported case [3, 19, 21, 26, 31, 32], there has been no study concerning the relationship between expression of cytotoxic molecules and the ultrastructure of cytotoxic granules. The aim of the present study was to compare the morphology of cytotoxic granules among nasal NK-cell lymphomas, intestinal T-cell lymphomas, and ALCLs.

Materials and methods

Case selection

Five cases of immunohistochemically and genetically defined nasal NK-cell lymphoma, two cases of intestinal T-cell lymphoma, and eight cases of ALCL were selected from the pathology files of Kawasaki Medical School Hospital between 1990 and present.

Cytology

Imprint preparations were made from fragments of the tumors. The specimens were smeared on glass slides by gentle touching. These were fixed in ethanol and stained with May–Giemsa staining. The number of cytoplasmic azurophilic granules was counted in one hundred lymphoma cells in each case under ×100 objective in oil immersion.

Flow cytometric analysis

Cell suspensions were obtained from fragments of the tumors by mincing and passing through the nylon mesh. They were examined by means of flow cytometry using a direct immunofluorescence method. The monoclonal antibodies (mAbs) used in this study were OKT11 (CD2, Ortho Pharmaceutical Co., Raritan, N.J.), OKT3 (CD3, Ortho), OKT4 (CD4, Ortho), Leu1 (CD5, Becton Dickinson, Mountain View, Calif.), OKT8 (CD8, Ortho), and NKH-1 (CD56, Coulter Immunology, Hialeah, Fla.).

Immunohistochemistry

For immunohistochemistry of frozen sections, tissues were embedded in Tissue Tek OTC compound (Miles, Naperville, Ill.) and then snap frozen in dry ice–acetone. Acetone-fixed, 6-μm sections were immunostained using an indirect method with the following mAbs: Leu12 (CD19; Becton-Dickinson; dilution 1:10), Leu4 (CD3; Becton-Dickinson; dilution 1:10), CD4 (CD4; Dako, Kyoto, Japan; dilution 1:10), OKT8 (CD8; Ortho; dilution 1:10), and Leu-7 (CD57; Becton-Dickinson; dilution 1:10).

For immunohistochemistry on paraffin sections, 4-μm cut paraffin sections were immunostained using an avidin-biotin horseradish peroxidase complex method, preceded by microwave antigen retrieval of tissue sections in a Dako antigen retrieval solution. The

Table 1 Summary of malignant lymphoma cases with cytotoxic phenotype examined in the present study. Imprint preparations were stained with May–Giemsa staining. + positive defined as antigen positivity >50%; – negative defined as antigen positivity <10%; *EBER-1* Epstein-Barr virus encoded RNA 1; *ALCL* anaplastic large cell lymphoma; *ALK* anaplastic lymphoma kinase; *TCL* T-cell lymphoma; *NKCL* natural killer cell lymphoma; *TIA-1* T-cell intracellular antigen 1; *TCR* T-cell receptor; *n.d.* not done

Case	Diagnosis	Age (years)/gender	Localization at presentation	Immunophenotype							Azurophilic granules[d]
				CD3[a]	CD4[a]	CD8[a]	CD56[b]	TIA-1[c]	Granzyme B[c]	EBER-1	
1	Nasal NKCL	72/Female	Nasal cavity	–	–	–	+	64	27	+	14±8
2	Nasal NKCL	43/Male	Nasal cavity, hard palate	–	–	–	+	61	13	+	10±4
3	Nasal NKCL	67/Male	Nasal cavity, maximal sinus	–	–	–	+	75	33	+	30±32
4	Nasal NKCL	78/Female	Nasal cavity	–	–	–	+	34	44	+	27±24
5	Nasal NKCL	26/Female	Nasal cavity, ethmoidal sinus	–	–	–	+	86	43	+	15±6
6	Intestinal TCL	43/Female	Jejunum, lung	+	–	+	+	91	45	–	40±15
7	Intestinal TCL	45/Female	Ileum	+	–	+	+	52	35	–	35±13
8	ALK^+ ALCL	20/Female	Lymph nodes	+	–	–	–	30	18	–	0±0
9	ALK^+ ALCL	29/Male	Vertebra	–	+	–	–	54	34	–	0±0
10	ALK^+ ALCL	26/Female	Lymph nodes	+	+	–	–	42	48	–	0±0
11	ALK^+ ALCL	35/Male	Lymph nodes	+	+	–	–	36	11	–	0±0
12	ALK^+ ALCL	23/Female	Lymph nodes	+	+	–	–	60	7	–	0±0
13	ALK^- ALCL	64/Male	Skin	+	+	–	–	22	10	–	0±0
14	ALK^- ALCL	20/Male	Lymph nodes	–	–	–	–	14	5	–	0±0
15	ALK^- ALCL	69/Male	Stomach	+	+	–	–	20	8	–	0±0

[a] Positivity was determined using flow cytometry and/or frozen section immunohistochemistry
[b] Positivity was determined using paraffin-section immunohistochemistry
[c] Percentage of positive lymphoma cells were determined in paraffin sections using immunohistochemistry as described in Materials and methods
[d] The number of azurophilic granules per cell (mean±SD, n=100)

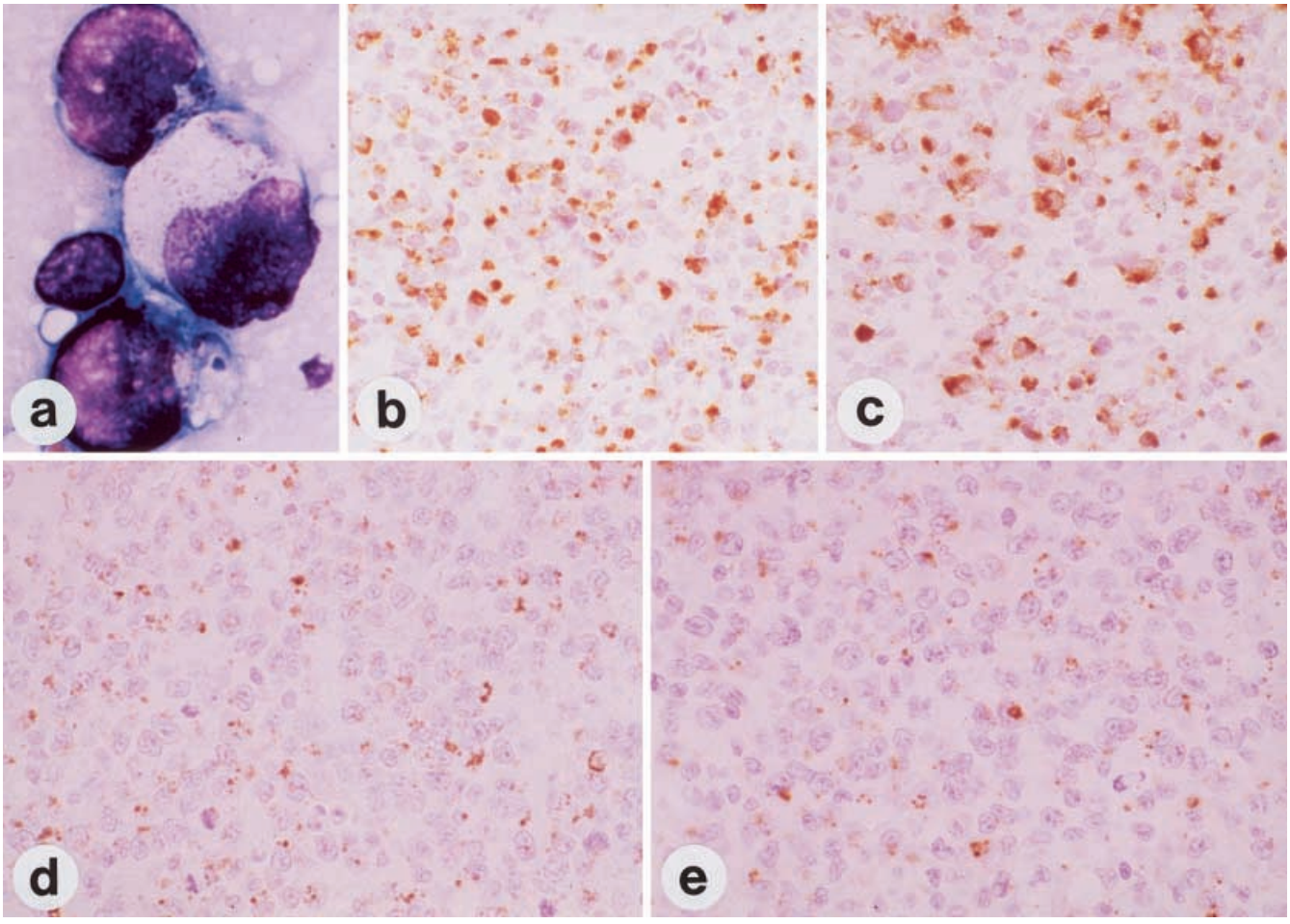

Fig. 1 **a** Cytologic pictures of fine azurophilic granules in tumor cells of natural killer (NK) cell lymphoma (case 3). Original magnification, ×500. **b** Expression of T-cell intracellular antigen 1 (TIA-1) in NK-cell lymphoma (case 5). Original magnification, ×100. **c** Expression of granzyme B in NK-cell lymphoma (case 5). Original magnification, ×100. **d** Expression of TIA-1 in anaplastic large cell lymphoma (ALCL; case 10). Original magnification, ×100. **e** Expression of granzyme B in ALCL (case 10). Original magnification, ×100

following antibodies were used: rabbit polyclonal anti-CD3ε antiserum (Dako; dilution 1:100), 123C3 (CD56; Zymed, San Francisco, Calif.; dilution 1:25), Leu-7 (CD57; Becton-Dickinson; dilution 1:10), GrB-7 (Granzyme B; Pharmacell, Paris, France; dilution 1:25), TIA-1 (TIA-1; Coulter; dilution 1:200), and ALK-1 (ALK; Dako; dilution 1:20). The sections were developed with diaminobenzidine and counterstained with hematoxylin. Negative controls were treated in the same manner but with the primary antibodies.

In situ hybridization of Epstein-Barr encoded RNA 1

In situ hybridization (ISH) was performed on the paraffin sections using a fluorescein isothiocyanate (FITC)-labeled Epstein-Barr encoded RNA 1 (EBER-1) 30-base oligonucleotide probe, as described previously [30]. Detection of the EBER-1 signal was carried out with an avidin-alkaline phosphatase conjugate, followed by a developing step using neufuscin as a substrate. A positive reaction was indicated by red coloring in the nucleus. The positive and negative controls consisted of a known Epstein-Barr virus (EBV)-positive nasopharyngeal carcinoma and a known EBV-negative lymph node, respectively.

Electron microscopy

The tissues were fixed in 2.5% glutaraldehyde and postfixed in 1% osmium tetroxide, routinely processed, and examined with an H-7000 electron microscope (Hitachi, Tokyo, Japan).

Immunoelectron microscopy

Tumor tissues from cases 4 and 12 were processed for post-embedding immunoelectron microscopy. The samples were fixed in 2% glutaraldehyde and embedded in LR white resin (London Resin Co., Reading, UK). After incubation in fetal bovine serum, ultrathin sections were incubated with anti-TIA-1 mAb (1:25 dilution) or isotype-matched control antibodies overnight at 4°C. They were then washed in phosphate-buffered saline (PBS) and reacted with 5 nm colloidal gold-conjugated rabbit anti-mouse immunoglobulin (Ig)G (1:10 dilution) for 45 min. After washing in PBS and post-fixation with glutaraldehyde, they were counterstained with uranyl acetate (case 4), or uranyl acetate and lead citrate (case 12) and observed using an H-7000 electron microscope (Hitachi, Tokyo, Japan).

DNA analysis

DNA was extracted from tumor tissues by treating them overnight with lysis buffer/proteinase K and extracting the mixture with phenol/chloroform. For rearrangement analysis, Southern blot hybrid-

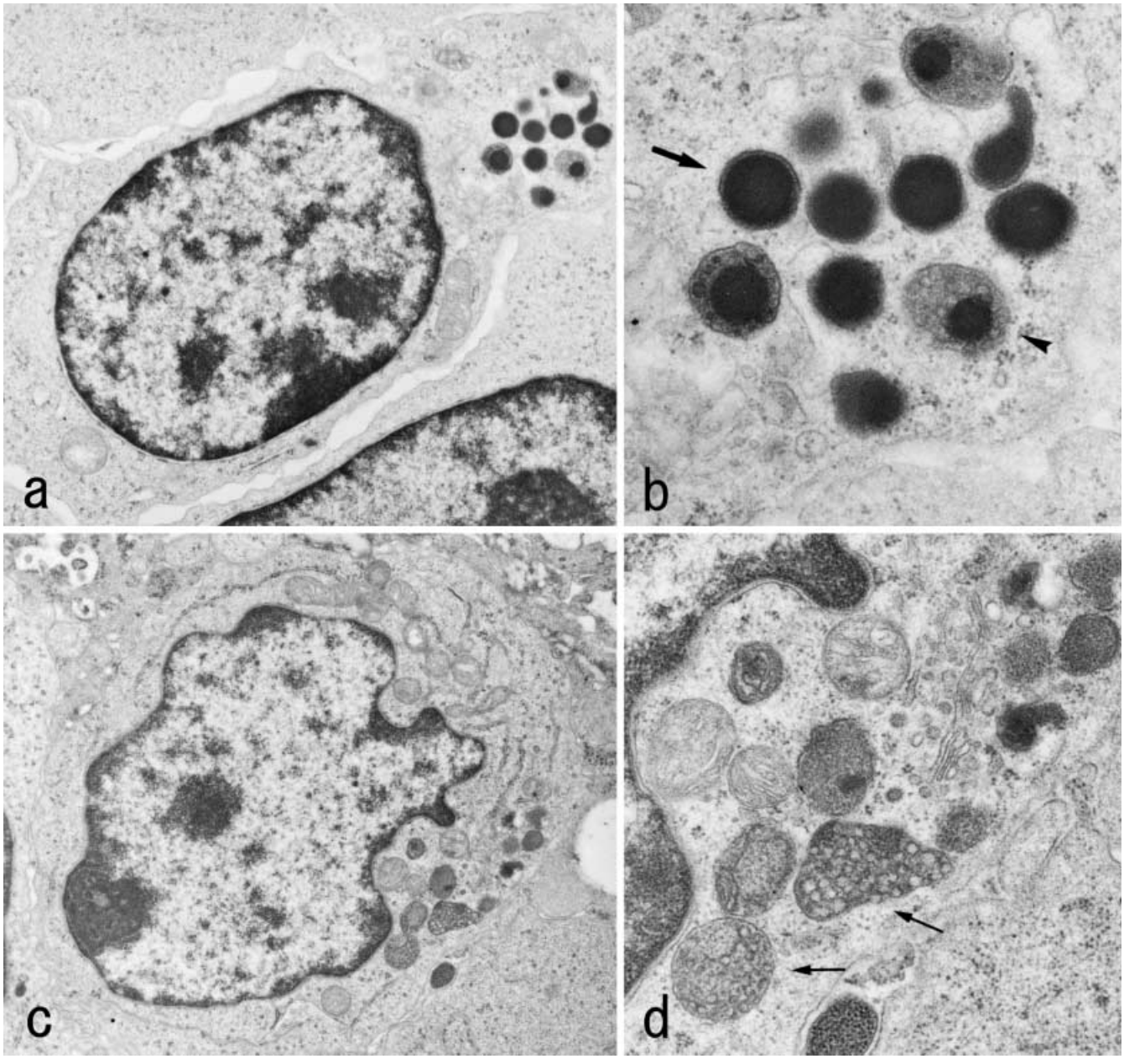

Fig. 2 Electron microscopy of nasal natural killer (NK) cell lymphoma. **a** Case 1. Intracytoplasmic granules were clustered to one side of the cytoplasm. Magnification, ×9000. **b** Case 1. Higher magnification (×33,000) of the cytoplasmic granules. *Arrow*, a dense core granule (type-I granule); *arrowhead*, an intermediate type granule. **c** Case 4. Cytoplasmic granules were located in the Golgi area. Magnification, ×9800. **d** Case 4. Higher magnification (×27,000) of various sizes of cytoplasmic granules. *Arrows*, multivesicular bodies (type-II granules)

ization was performed to detect the T-cell receptor (TCR) β-, γ-, and δ-chain genes. DNA (5 μg) was digested with restriction endonucleases, separated by electrophoresis in 0.8% agarose gel and then transferred to activated nylon membranes. The DNA fragments on the membranes were hybridized with nick-translated ^{32}P-labeled probes, and examined using autoradiography. The restriction endonucleases used were *Bam*HI or *Eco*RV for the TCR-Cβ1, *Eco*RI or *Bam*HI, or *Hind* III for TCR-Jγ, and *Bgl*II or *Hind*III for the TCR-Jδ1.

Statistics

Significance was calculated using Students *t* test. *P* values <0.05 were considered significant.

Results

The clinical and cytological findings of 15 cases examined in the present study are summarized in Table 1.

Nasal NK-cell lymphoma

All five nasal NK-cell lymphoma cases showed identical phenotypes: azurophilic granules$^+$ (Fig. 1a), CD2$^+$, CD3$^-$, CD3ε$^+$, CD5$^-$, CD56$^+$, TIA-1$^+$ (Fig. 1b), gran-

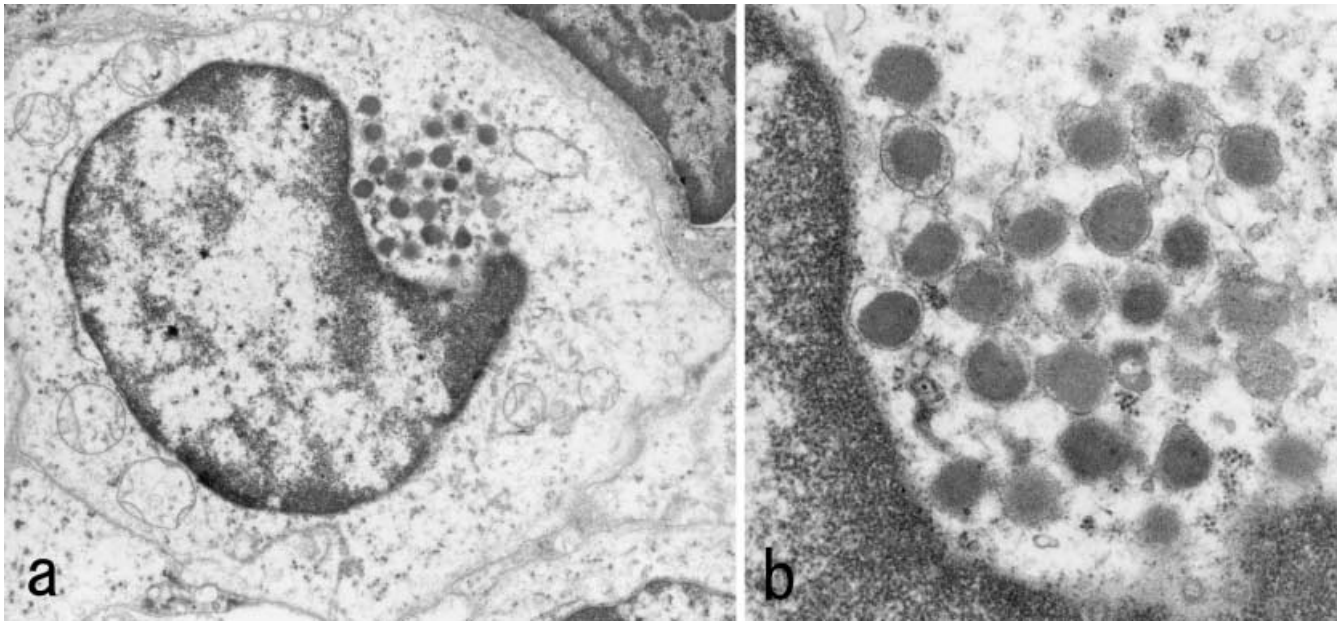

Fig. 3 Electron microscopy of intestinal T-cell lymphoma (case 6). **a** Cytoplasmic granules were located around the Golgi complex. Magnification, ×9300. **b** The cytoplasmic granules were mostly type-I granules. Magnification, ×28,000

zyme B^+ (Fig. 1c), and EBER-1^+. No case showed TCR rearrangement. The number of azurophilic granules in a lymphoma cell varied in each case (mean±SD, 19.2±8.8; Table 1). Ultrastructurally, nuclei of the lymphoma cells were irregular and contained large distinct nucleoli. The cytoplasm contained well-developed Golgi complex, mitochondria, rough endoplasmic reticulum, and cytoplasmic granules. The morphology of the cytoplasmic granules varied among cases, but there were two distinct types clustered in the peripheral cytoplasm or located around the Golgi complex (Fig. 2a, c). Type-I granules ranged in size from 160 nm to 890 nm and had a dense core surrounded by a thin membrane. Most were rounded (Fig. 2b). Type-II granules ranged from 280 nm to 1100 nm and contained 50-nm sized multiple small vesicles packed in the membrane (Fig. 2d). Also recognized were intermediate form granules (220~660 nm) characterized by both features of dense core and multiple vesicles (Fig. 2b, d). Inclusions of tubular structures in a parallel array, which were described in human large granular lymphocytes [18], were not found in any case.

Intestinal T-cell lymphoma

The two intestinal T-cell lymphoma cases were histologically monomorphic medium-sized lymphomas. They were positive for CD3, CD3ε, CD56, CD8, TIA-1, and granzyme B but negative for CD4 and CD5. Case 6 showed rearrangement of TCR Cβ1 and Jγ, and deletion of Jδ1 by means of Southern blotting. Upon Giemsa staining, lymphoma cells had azurophilic granules in clear cytoplasm. Ultrastructurally, cytoplasmic granules predominantly clustered in the Golgi area (Fig. 3a). In case 6, most of the granules were type-I and were relatively uniform in size (300 nm; Fig. 3b). In case 7, the shape and size of type-I granules were more variable in each lymphoma cell compared with those of case 6 (not shown).

Anaplastic large cell lymphoma

All cases were positive for CD30. CD4 expression was demonstrated in lymphoma cells in six cases. There was no case with CD8 and/or CD56 expression. Rearrangement of TCR Cβ1 was demonstrated only in case 8 by means of Southern blotting. Upon Giemsa staining, no azurophilic granules were found in any case. Immunohistochemically, however, tumor cells of these cases were positive for TIA-1 and granzyme B (Fig. 1d, e). The percentage of TIA-1 positive cells in the ALCLs was significantly fewer than that in nasal NK-cell lymphomas (34.8±16.5% vs 64.0±19.5%, $P<0.05$). The percentage of granzyme B positive cells also had a significant difference between the ALCLs and NK-cell lymphomas (17.6±15.4% vs 32.0±12.8%, $P<0.05$). At the ultrastructural level, the cytoplasm contained a variable number of polyribosomes, a few mitochondria, and rare lipid vacuoles (Fig. 4a). Interestingly, all cases had type-II granules consisting of multiple small vesicles, which ranged from 150 nm to 750 nm (Fig. 4b–d). These granules were present singly in the cytoplasm or clustered in the Golgi area and frequently associated with mitochondria. In cases 13 and 14, type-II granules were rarely found. Type-I granules were not seen in any case.

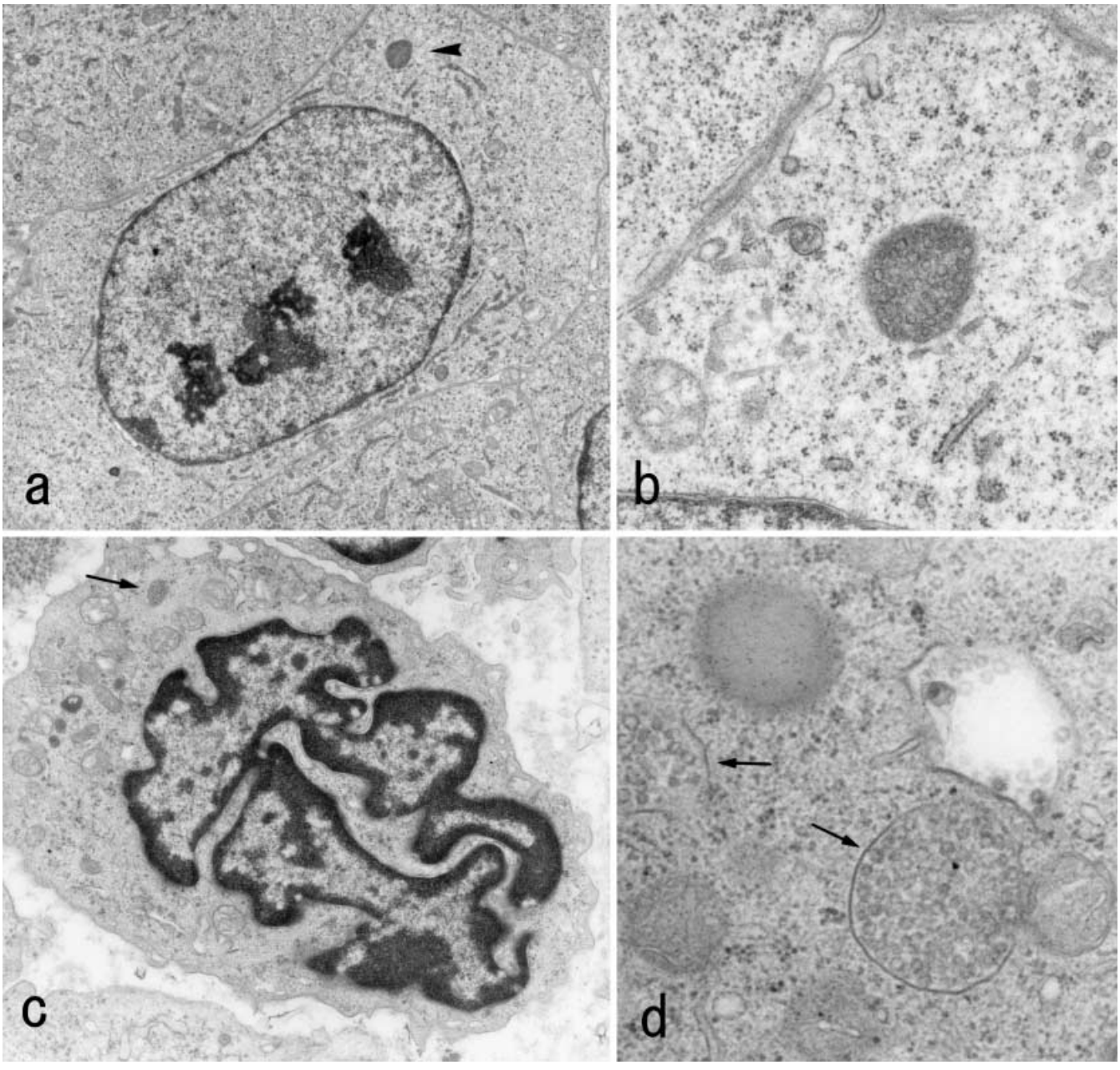

Fig. 4 Electron microscopy of anaplastic large cell lymphoma (ALCL). **a** Case 9. The lymphoma cell had an oval nucleus. Note a type-II granule (multivesicular body) singly located (*arrowhead*). Magnification, ×6300. **b** Case 9. Higher magnification (×38,000) of the type-II granule. **c** Case 13. The lymphoma cell had a bizarre nucleus. Note a type-II granule (multivesicular body) singly located (*arrow*). Magnification, ×10,300. **d** Case 13. Type-II granules similar to those of natural killer cell lymphoma (*arrows*). Magnification, ×40,000

Immunoelectron microscopy of TIA-1

Ultrastructural distribution of TIA-1 was studied in a case of NK-cell lymphoma (case 4) and a case of ALCL (case 12) using the post-embedding method of immunoelectron microscopy. TIA-1 immunolabeling was primarily located at the periphery of the cytoplasmic granules in ALCL and NK-cell lymphoma (Fig. 5).

Discussion

In the present study, NK-cell lymphoma and intestinal T-cell lymphoma had type-I and type-II cytotoxic granules, whereas ALCL had only type-II granules. Thus, malignant lymphomas with the cytotoxic phenotype can be divided into type-I granule-positive and type-I granule-negative lymphomas. Krenacs et al. failed to find cytotoxic granules in their cases of ALCL with expression of cytotoxic proteins, granzyme B, and TIA-1 [23]. Their findings were consistent with those from previous ultrastructural studies on ALCL [22, 25, 35]. In contrast,

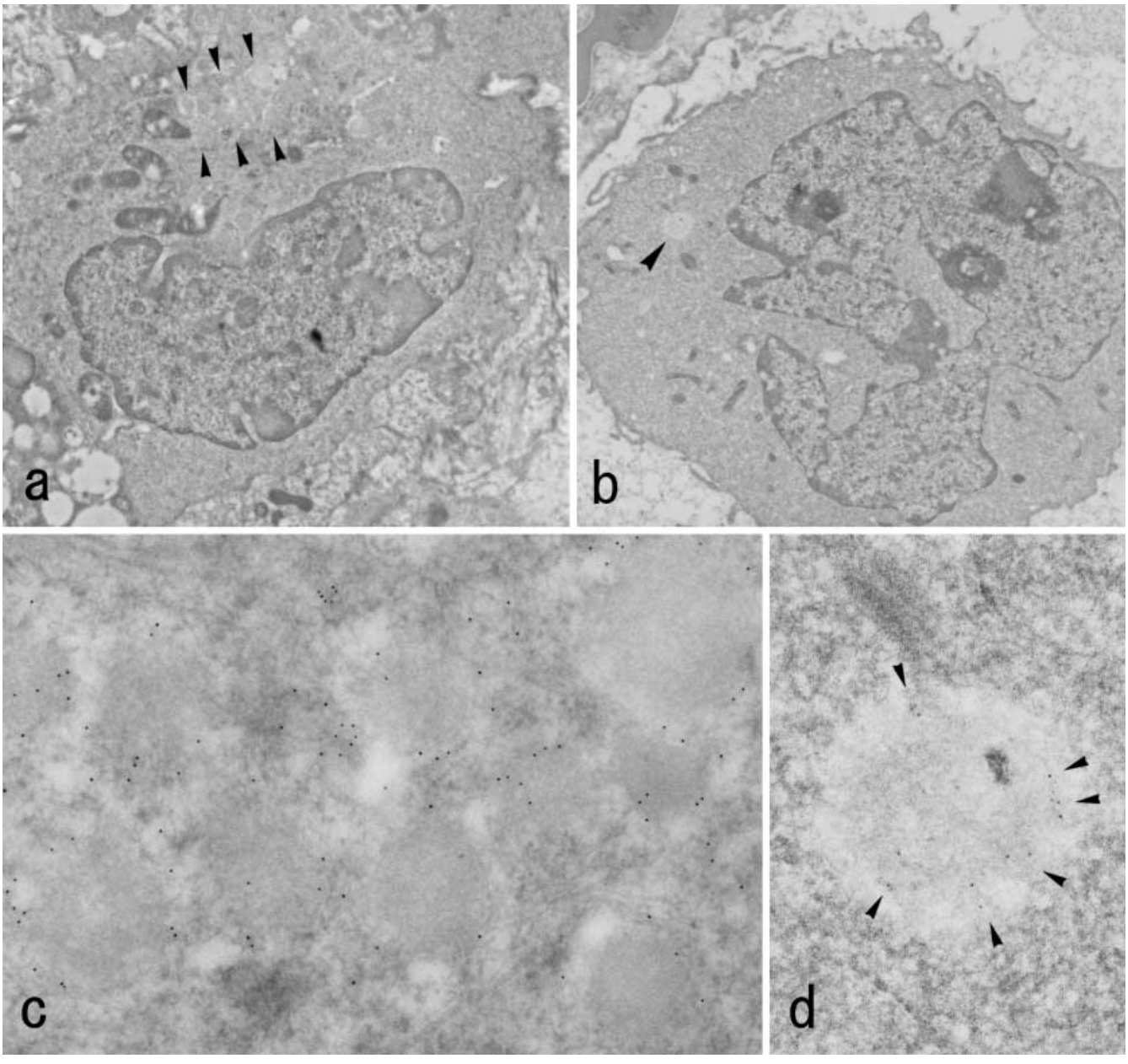

Fig. 5 Immunoelectron microscopy of T-cell intracellular antigen 1 (TIA-1). **a** Natural killer (NK) cell lymphoma (case 4). Positively labeled intracytoplasmic granules (*arrowheads*) were clustered to one side of the cytoplasm. Magnification, ×12,000. **b** Anaplastic large cell lymphoma (ALCL; case 15). Positively labeled intracytoplasmic granule was singly located (*arrowhead*). Magnification, ×7500. **c** Higher magnification of **a**. Gold colloid particles were primarily located at the periphery of cytoplasmic granules corresponding to type I granules. Magnification, ×100,000. **d** Higher magnification of **c**. Gold colloid particles (*arrowheads*) were located at the cytoplasmic granule corresponding to type-II granule. Magnification, ×100,000

Felgar et al. recently reported that both type-I and type-II granules were present in four of four ALCL cases examined ultrastructurally [14]. Thus, the issue regarding cytotoxic granules in ALCL appears controversial.

The present finding that all cases of ALCL with cytotoxic proteins lacked type-I granules but had type-II granules suggests that ALCL can be separated from NK-cell lymphoma based on the lack of type-I granules. Although the reason for the discrepancy between the ultrastructural studies of ALCLs is not clear, one possibility is that the cases of Felgar et al. might have included different types of ALCLs, which were not included in the present study. Indeed, four of 12 TIA-1-positive ALCL cases were positive for CD56 in their study, whereas no CD56-positive ALCL cases were included in the present study. In this regard, we cannot exclude the possibility that their patient population and/or diagnostic criteria were significantly different from the present study.

TIA-1 was initially shown to be predominantly located on the cytoplasmic face of the outer limiting mem-

branes of type-I and type-II granules [1, 2]. This localization pattern of TIA-1 was confirmed in the present cases of NK-cell lymphoma and ALCL using immunoelectron microscopy.

Type-II granules probably correspond to prelysosomes because they have been shown to contain lysosomal proteins, including acid phosphatase in NK cells [5]. In ALCL, this structure was more frequently found in ALK-positive ALCL than in ALK-negative ALCL. This finding is paralleled by a lower expression of TIA-1 and granzyme B in ALK-negative ALCL. Since the expression of cytotoxic proteins has been found unrelated to clinical outcome of ALCL [11], the presence of type-II granules does not appear to have any impact on the evaluation of aggressiveness of the lymphoma.

Since NK-cell lymphoma cells can retain cytotoxic function to induce apoptosis of tissue cells [19, 33], this function may be associated with the clinical aggressiveness of this type of lymphoma [24]. $CD56^+$ intestinal T-cell lymphoma is most likely derived from activated cytotoxic intraepithelial T lymphocytes [6]. Patients with this lymphoma show a high incidence of perforation at initial presentation and usually follow an aggressive clinical course [6]. In this respect, the presence of complete sets of cytotoxic granules in aggressive lymphoma, such as nasal NK-cell lymphomas and $CD56^+$ intestinal T-cell lymphomas, is quite intriguing, because type-I cytotoxic granules are essential for the lymphoma cells to exert a cytotoxic function. From the present study, however, it appears difficult to draw a definitive conclusion that the presence of type-I granules is a morphological indicator for the aggressiveness of cytotoxic lymphomas, because the number cases and the type of lymphoma examined were limited. Further ultrastructural studies on cytotoxic granules in a greater number of lymphoma cases expressing cytotoxic molecules should clarify this point.

In conclusion, we described the morphological characteristics of cytotoxic granules of nasal NK-cell lymphoma, $CD56^+$ intestinal T-cell lymphoma, and ALCL. The present findings may contribute to our further understanding of the clinicopathological differences among malignant lymphomas with cytotoxic phenotypes.

Acknowledgement This study was supported by a Project Grant (11–603) from Kawasaki Medical School.

References

1. Anderson P (1995) TIA-1: structural and functional studies on a new class of cytolytic effector molecule. Curr Top Microbiol Immunol 198:131–143
2. Anderson P, Nagler-Anderson C, O'Brien C, Levine H, Watkins S, Slayter HS, Blue ML, Schlossman SF (1990) A monoclonal antibody reactive with a 15-kDa cytoplasmic granule-associated protein defines a subpopulation of CD8+ T lymphocytes. J Immunol 144:574–582
3. Berti E, Cerri A, Cavicchini S, Delia D, Soligo D, Alessi E, Caputo R (1991) Primary cutaneous gamma/delta T-cell lymphoma presenting as disseminated pagetoid reticulosis. Invest Dermatol 96:718–723
4. Boulland ML, Kanavaros P, Wechsler J, Casiraghi O, Gaulard P (1997) Cytotoxic protein expression in natural killer cell lymphomas and in alpha beta and gamma delta peripheral T cell lymphomas. J Pathol 183:432–439
5. Burkhardt JK, Hester S, Lapham CK, Argon Y (1990) The lytic granules of natural killer cells are dual-function organelles combining secretory and pre-lysosomal compartments. J Cell Biol 111:2327–2340
6. Chott A, Haedicke W, Mosberger I, Fodinger M, Winkler K, Mannhalter C, Muller-Hermelink H (1998) Most CD56+ intestinal lymphoma are CD8+CD5- T-cell lymphomas of monomorphic small to medium size histology. Am J Pathol 153:1483–1490
7. Chott A, Vesely M, Simonitsch I, Mosberger I, Hanak H (1999) Classification of intestinal T-cell neoplasms and their differential diagnosis. Am J Clin Pathol:111[Suppl 1]:68–74
8. Darmon AJ, Nicholson DW, Bleackley RC (1995) Activation of apoptotic protease CPP32 by cytotoxic T-cell-derived granzyme B. Nature 377:446–448
9. Daum S, Foss H, Anagnostopoulos I, Dederke B, Demel G, Araujo I, Riecken E, Stein H, the German study group on intestinal non-Hodgkin lymphoma (1997) Expression of cytotoxic molecules in intestinal T-cell lymphomas. J Pathol 182:311–317
10. De Bruin PC, Kummer JA, Van der Valk P, Van Heerde P, Kluin PM, Willemze R, Ossenkoppele GJ, Radaszkiewicz T, Meijer CJLM (1994) Granzyme B-expressing peripheral T-cell lymphomas: neoplastic equivalents of activated cytotoxic T cells with preference for mucosa-associated lymphoid tissue localization. Blood 84:3785–3791
11. Dukers DF, ten Berge RL, Oudejans JJ, Pulford K, Hayes D, Misere JF, Ossenkoppele GJ, Jaspars LH, Willemze R, Meijer CJ (1999) A cytotoxic phenotype does not predict clinical outcome in anaplastic large cell lymphomas. J Clin Pathol 52:129–136
12. Falini B, Pileri S, Zinzani PL, Carbone A, Zagonel V, Wolf-Peeters C, Verhoef G, Menestrina F, Todeschini G, Paulli M, Lazzarino M, Giardini R, Aiello A, Foss HD, Araujo I, Fizzotti M, Pelicci PG, Flenghi L, Martelli MF, Santucci A (1999) ALK+ lymphoma: clinico-pathological findings and outcome. Blood 93:2697–2706
13. Felgar RE, Macon WR, Kinney MC, Roberts S, Pasha T, Salhany KE (1997) TIA-1 expression in lymphoid neoplasms. Identification of subsets with cytotoxic T lymphocyte or natural killer cell differentiation. Am J Pathol 150:1893–1900
14. Felgar RE, Salhany KE, Macon WR, Pietra GG, Kinny MC (1999) The expression of TIA-1+ cytolytic-type granules and other cytotolytic lymphocyte-associated markers in CD30+ anaplastic large cell lymphomas (ALCL): Correlation with morphology, immunophenotype, ultrastructure, and clinical features. Hum Pathol 30:228–236
15. Foss HD, Anagnostopoulos I, Araujo I, Assaf C, Demel G, Kummer JA, Hummel M, Stein H (1996) Anaplastic large-cell lymphomas of T cell and null-cell phenotype express cytotoxic molecules. Blood 88:4005–4011
16. Griffiths GM, Argon Y (1995) Structure and biogenesis of lytic granules. Curr Top Microbiol Immunol 198:39–58
17. Hahn S, Gehri R, Erb P (1995) Mechanism and biological significance of CD4-mediated cytotoxicity. Immunol Rev 146:57–79
18. Huhn D, Huber C, Gastl G (1982) Large granular lymphocytes: morphological studies. Eur J Immunol 12:985–988
19. Imamura N, Kusunoki Y, Kawa-Ha K, Yumura K, Hara J, oda K, Abe K, Dohy H, Inada T, Kajihara H, Kuramoto A (1990) Aggressive natural killer cell leukemia/lymphoma: report of four cases and review of the literature. Brit J Haematol 75:49–59
20. Jaffe ES, Chan JK (1996) Report of the workshop on nasal and related extranodal angiocentric T/natural killer cell lymphomas. Am J Surg Pathol 20:103–111

21. Kanavaros P, Lavergne A, Galian A, Boivin P, Fourmestreaux AR, Priollet BC, Flandrin G, Hautefeuille P (1988) A primary immunoblastic T malignant lymphoma of the small bowel, with azurophilic intracytoplasmic granules. A histologic, immunologic, and electron microscopy study. Am J Surg Pathol 12:641–647
22. Kinney MC, Greer JP, Glick AD, Salhany KE, Collins RD (1991) Anaplastic large-cell Ki-1 malignant lymphomas. Recognition, biological and clinical implications. Pathol Annu 26:1–24
23. Krenacs L, Wellmann A, Sorbara L, Himmelmann AW, Bagdi E, Jaffe ES, Raffeld M (1997) Cytotoxic cell antigen expression in anaplastic large cell lymphomas of T- and null-cell type and Hodgkin's disease: evidence for distinct cellular origin. Blood 89:980–989
24. Kwong YL, Chan AC, Liang RH (1997) Natural killer cell lymphoma/leukemia: pathology and treatment. Hematol Oncol 15:71–79
25. Le Tourneau A, Audouin J, Diebold J (1988) Ultrastructural study of 4 cases of Ki-1 positive large anaplastic cell malignant lymphoma. Virchows Arch 413:215–222
26. Macon WR, Williams ME, Greer JP, Hammer RD, Glick AD, Collins RD, Cousar JB (1996) Natural killer-like T cell lymphomas: aggressive lymphomas of T-large granular lymphocytes. Blood 87:1474–1483
27. Nakamura S, Shiota M, Nakagawa A, Yatabe Y, Kojima M, Motoori T, Suzuki R, Kagami Y, Ogura M, Morishima Y, Mizoguchi Y, Okamoto M, Seto M, Koshikawa T, Mori S, Suchi T (1997) Anaplastic large cell lymphoma: a distinct molecular pathologic entity: a reappraisal with special reference to p80 (NPM/ALK) expression. Am J Surg Pathol 21:1420–1432
28. Neighbour PA, Huberman HS, Kress Y (1982) Human large granular lymphocytes and natural killing: ultrastructural studies of strontium-induced degranulation. Eur J Immunol 12:588–595
29. Peters PJ, Borst J, Oorschot V, Fukuda M, Krahenbuhl O, Tschopp J, Slot JW, Geuze HJ (1991) Cytotoxic T lymphocyte granules are secretory lysosomes, containing both perforin and granzymes. J Exp Med 173:1099–1109
30. Sadahira Y, Ohmoto K, Yamamoto S, Nishihara H, Wada H, Yawata Y, Manabe T (1998) Expression of cytotoxic molecule TIA-1 in malignant lymphomas mimicking fulminant hepatitis. Pathol Int 48:695–705
31. Salhany KE, Feldman M, Kahn MJ, Peritt D, Schretzenmair RD, Wilson DM, Dipaola RS, Glick AD, Kant JA, Nowell PC, Kamoun M (1997) Hepatosplenic γδ T cell lymphoma: ultrastructural, immunophenotypic, and functional evidence for cytotoxic T lymphocyte differentiation. Hum Pathol 28:674–685
32. Takeshita M, Kimura N, Suzumiya J, Ohshima K, Kikuchi M, Watanabe R, Okamura T, Goto H (1994) Angiocentric lymphoma with granulomatous panniculitis in the skin expressing natural killer cell and large granular T-cell phenotypes. Virchows Arch 425:499–504
33. Tsuchiyama J, Yoshino T, Mori M, Kondoh E, Oka T, Akagi T, Hiraki A, Nakayama H, Shibuya A, Ma Y, Kawabata T, Okada S, Harada M (1998) Characterization of a novel human natural killer-cell line (NK-YS) established from natural killer cell lymphoma/leukemia associated with Epstein-Barr virus infection. Blood 92:1374–383
34. Young JD, Hengartner H, Podack ER, Cohn ZA (1986) Purification and characterization of a cytolytic pore-forming protein from granules of cloned lymphocytes with natural killer activity. Cell 44:849–859
35. Yowell R, Hammond E (1992) Ki-1 lymphoma: a case report. Ultrastruct Pathol 16:11–16